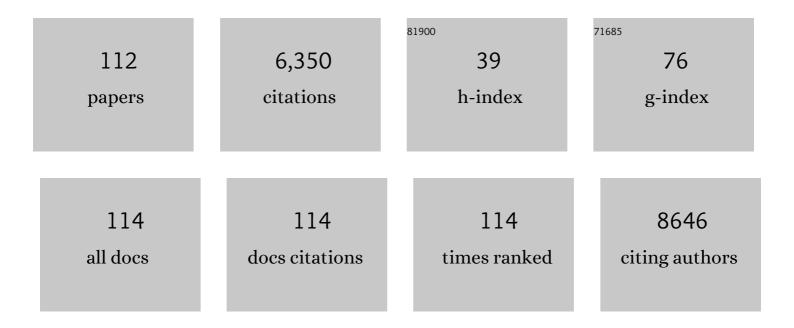


List of Publications by Year in descending order

Source: https://exaly.com/author-pdf/1881749/publications.pdf Version: 2024-02-01



Vinili

#	Article	IF	CITATIONS
1	Cocatalysts for Selective Photoreduction of CO ₂ into Solar Fuels. Chemical Reviews, 2019, 119, 3962-4179.	47.7	1,591
2	A Graphene-like Oxygenated Carbon Nitride Material for Improved Cycle-Life Lithium/Sulfur Batteries. Nano Letters, 2015, 15, 5137-5142.	9.1	358
3	High-performance all-solid state asymmetric supercapacitor based on Co3O4 nanowires and carbon aerogel. Journal of Power Sources, 2015, 282, 179-186.	7.8	269
4	High flux electroneutral loose nanofiltration membranes based on rapid deposition of polydopamine/polyethyleneimine. Journal of Materials Chemistry A, 2017, 5, 14847-14857.	10.3	195
5	Dimensionâ€Matched Zinc Phthalocyanine/BiVO ₄ Ultrathin Nanocomposites for CO ₂ Reduction as Efficient Wideâ€Visibleâ€Lightâ€Driven Photocatalysts via a Cascade Charge Transfer. Angewandte Chemie - International Edition, 2019, 58, 10873-10878.	13.8	168
6	Synthesis of core-shell magnetic molecular imprinted polymer by the surface RAFT polymerization for the fast and selective removal of endocrine disrupting chemicals from aqueous solutions. Environmental Pollution, 2010, 158, 2317-2323.	7.5	167
7	A graphene oxide-based molecularly imprinted polymer platform for detecting endocrine disrupting chemicals. Carbon, 2010, 48, 3427-3433.	10.3	157
8	Computational design and synthesis of molecular imprinted polymers with high selectivity for removal of aniline from contaminated water. Analytica Chimica Acta, 2008, 610, 282-288.	5.4	102
9	Surface molecular imprinting onto fluorescein-coated magnetic nanoparticlesvia reversible addition fragmentation chain transfer polymerization: A facile three-in-one system for recognition and separation of endocrine disrupting chemicals. Nanoscale, 2011, 3, 280-287.	5.6	96
10	The preparation and drug delivery of a graphene–carbon nanotube–Fe3O4 nanoparticle hybrid. Journal of Materials Chemistry B, 2013, 1, 2658.	5.8	96
11	An investigation on the photoelectrochemical properties of dye-sensitized solar cells based on graphene–TiO2 composite photoanodes. Journal of Power Sources, 2014, 262, 349-355.	7.8	96
12	Ethyl acetate green antisolvent process for high-performance planar low-temperature SnO2-based perovskite solar cells made in ambient air. Chemical Engineering Journal, 2020, 379, 122298.	12.7	95
13	Bio-inspired co-deposited preparation of GO composite loose nanofiltration membrane for dye contaminated wastewater sustainable treatment. Journal of Hazardous Materials, 2020, 400, 123121.	12.4	95
14	Selective recognition and removal of chlorophenols from aqueous solution using molecularly imprinted polymer prepared by reversible addition-fragmentation chain transfer polymerization. Biosensors and Bioelectronics, 2009, 25, 306-312.	10.1	92
15	Graphene oxide shell-isolated Ag nanoparticles for surface-enhanced Raman scattering. Carbon, 2015, 81, 767-772.	10.3	91
16	Effect of preferential exposure of anatase TiO2 {0 0 1} facets on the performance of Mn-Ce/TiO2 catalysts for low-temperature selective catalytic reduction of NOx with NH3. Chemical Engineering Journal, 2019, 369, 26-34.	12.7	90
17	Multiply Wrapped Porphyrin Dyes with a Phenothiazine Donor: A High Efficiency of 11.7% Achieved through a Synergetic Coadsorption and Cosensitization Approach. ACS Applied Materials & Interfaces, 2019, 11, 5046-5054.	8.0	83
18	Selective removal of 2,4-dichlorophenol from contaminated water using non-covalent imprinted microspheres. Environmental Pollution, 2009, 157, 1879-1885.	7.5	76

#	Article	IF	CITATIONS
19	Selective recognition of veterinary drugs residues by artificial antibodies designed using a computational approach. Biomaterials, 2009, 30, 3205-3211.	11.4	70
20	O doping hierarchical NiCoP/Ni2P hybrid with modulated electron density for efficient alkaline hydrogen evolution reaction. Applied Catalysis B: Environmental, 2021, 293, 120196.	20.2	67
21	Limitations of MTT and CCK-8 assay for evaluation of graphene cytotoxicity. RSC Advances, 2015, 5, 53240-53244.	3.6	65
22	D-A-π-A based organic dyes for efficient DSSCs: A theoretical study on the role of π-spacer. Computational Materials Science, 2019, 161, 163-176.	3.0	65
23	Preparation and magnetic property of multiwalled carbon nanotubes decorated by Fe3O4 nanoparticles. New Carbon Materials, 2012, 27, 111-116.	6.1	63
24	Synthesis and properties of core-shell magnetic molecular imprinted polymers. Applied Surface Science, 2012, 258, 6660-6664.	6.1	59
25	Development of a model for the rational design of molecular imprinted polymer: Computational approach for combined molecular dynamics/quantum mechanics calculations. Analytica Chimica Acta, 2009, 647, 117-124.	5.4	58
26	Surface molecular imprinting onto silver microspheres for surface enhanc24 June 2013ed Raman scattering applications. Biosensors and Bioelectronics, 2013, 50, 106-110.	10.1	57
27	Design of Ni ₃ N/Co ₂ N heterojunctions for boosting electrocatalytic alkaline overall water splitting. Journal of Materials Chemistry A, 2021, 9, 10260-10269.	10.3	57
28	Preparation of core-shell molecularly imprinted polymer via the combination of reversible addition-fragmentation chain transfer polymerization and click reaction. Analytica Chimica Acta, 2010, 680, 65-71.	5.4	56
29	Controlling Interfacial Recombination in Aqueous Dyeâ€Sensitized Solar Cells by Octadecyltrichlorosilane Surface Treatment. Angewandte Chemie - International Edition, 2014, 53, 6933-6937.	13.8	55
30	Silver microspheres coated with a molecularly imprinted polymer as a SERS substrate for sensitive detection of bisphenol A. Mikrochimica Acta, 2018, 185, 242.	5.0	55
31	Improved the long-term air stability of ZnO-based perovskite solar cells prepared under ambient conditions via surface modification of the electron transport layer using an ionic liquid. Electrochimica Acta, 2018, 268, 539-545.	5.2	49
32	An easy and novel approach for the decoration of graphene oxide by Fe3O4 nanoparticles. Applied Surface Science, 2011, 257, 6059-6062.	6.1	48
33	High performance surface-enhanced Raman scattering from molecular imprinting polymer capsulated silver spheres. Physical Chemistry Chemical Physics, 2015, 17, 21343-21347.	2.8	48
34	Preparation of graphene oxide–molecularly imprinted polymer composites via atom transfer radical polymerization. Journal of Materials Science, 2011, 46, 2024-2029.	3.7	47
35	Spin-assisted interfacial polymerization strategy for graphene oxide-polyamide composite nanofiltration membrane with high performance. Applied Surface Science, 2020, 508, 145198.	6.1	46
36	Multifunctional imprinted polymers based on CdTe/CdS and magnetic graphene oxide for selective recognition and separation of p-t-octylphenol. Chemical Engineering Journal, 2015, 271, 87-95.	12.7	45

#	Article	IF	CITATIONS
37	An Er-doped TiO ₂ phase junction as an electron transport layer for efficient perovskite solar cells fabricated in air. Journal of Materials Chemistry A, 2018, 6, 15348-15358.	10.3	42
38	Millisecond-pulsed photonically-annealed tin oxide electron transport layers for efficient perovskite solar cells. Journal of Materials Chemistry A, 2017, 5, 24110-24115.	10.3	41
39	A Numerical Simulation and Impedance Study of the Electron Transport and Recombination in Binder-Free TiO ₂ Film for Flexible Dye-Sensitized Solar Cells. Journal of Physical Chemistry C, 2008, 112, 13744-13753.	3.1	40
40	Flexible asymmetric supercapacitor with high energy density based on optimized MnO2 cathode and Fe2O3 anode. Chinese Chemical Letters, 2019, 30, 750-756.	9.0	39
41	A core–shell Fe3O4 nanoparticle–CdTe quantum dot–molecularly imprinted polymer composite for recognition and separation of 4-nonylphenol. Analytical Methods, 2014, 6, 2855.	2.7	38
42	Temperature-directed synthesis of N-doped carbon-based nanotubes and nanosheets decorated with Fe (Fe ₃ O ₄ , Fe ₃ C) nanomaterials. Nanoscale, 2019, 11, 9155-9162.	5.6	37
43	First-Principles Investigation on Electronic Properties of Quantum Dot-Sensitized Solar Cells Based on Anatase TiO2 Nanotubes. Journal of Physical Chemistry C, 2011, 115, 20307-20315.	3.1	36
44	Theoretical screening of high-efficiency sensitizers with D-Ï€-A framework for DSSCs by altering promising donor group. Solar Energy, 2020, 196, 146-156.	6.1	35
45	Titania nanobundle networks as dye-sensitized solar cell photoanodes. Nanoscale, 2014, 6, 3704-3711.	5.6	34
46	A strategy toward air-stable and high-performance ZnO-based perovskite solar cells fabricated under ambient conditions. Chemical Engineering Journal, 2018, 336, 732-740.	12.7	32
47	A Ag-molecularly imprinted polymer composite for efficient surface-enhanced Raman scattering activities under a low-energy laser. Analyst, The, 2015, 140, 3239-3243.	3.5	30
48	The integration of molecular imprinting and surface-enhanced Raman scattering for highly sensitive detection of lysozyme biomarker aided by density functional theory. Spectrochimica Acta - Part A: Molecular and Biomolecular Spectroscopy, 2020, 228, 117764.	3.9	30
49	Surfactant Sodium Dodecyl Benzene Sulfonate Improves the Efficiency and Stability of Airâ€Processed Perovskite Solar Cells with Negligible Hysteresis. Solar Rrl, 2020, 4, 2000376.	5.8	30
50	Synthesis of dense MoS ₂ nanosheet layers on hollow carbon spheres and their applications in supercapacitors and the electrochemical hydrogen evolution reaction. Inorganic Chemistry Frontiers, 2018, 5, 2198-2204.	6.0	29
51	Ultraviolet-ozone modification on TiO2 surface to promote both efficiency and stability of low-temperature planar perovskite solar cells. Chemical Engineering Journal, 2020, 393, 124731.	12.7	29
52	Investigation of the catalytic activity for ozonation on the surface of NiO nanoparticles. Chemical Physics Letters, 2009, 479, 310-315.	2.6	28
53	Fluorescent features of CdTe nanorods grafted to graphene oxide through an amidation process. Journal of Materials Chemistry, 2011, 21, 11283.	6.7	27
54	The application of hollow box TiO2 as scattering centers in dye-sensitized solar cells. Journal of Power Sources, 2016, 333, 10-16.	7.8	26

#	Article	IF	CITATIONS
55	A NH4F interface passivation strategy to produce air-processed high-performance planar perovskite solar cells. Electrochimica Acta, 2018, 282, 653-661.	5.2	26
56	High performance surface-enhanced Raman scattering via dummy molecular imprinting onto silver microspheres. Chemical Communications, 2014, 50, 14331-14333.	4.1	25
57	Preparation of hierarchical rutile TiO2 microspheres as scattering centers for efficient dye-sensitized solar cells. Electrochimica Acta, 2017, 255, 187-194.	5.2	24
58	Fabrication of peanut-like TiO2 microarchitecture with enhanced surface light trapping and high specific surface area for high-efficiency dye sensitized solar cells. Journal of Power Sources, 2019, 423, 236-245.	7.8	24
59	One-step implementation of plasmon enhancement and solvent annealing effects for air-processed high-efficiency perovskite solar cells. Journal of Materials Chemistry A, 2018, 6, 24036-24044.	10.3	23
60	HClO4-assisted fabrication of SnO2/C60 bilayer electron-transport materials for all air-processed efficient and stable inverted planar perovskite solar cells. Journal of Power Sources, 2020, 476, 228648.	7.8	23
61	Carboxyl functional group-assisted defects passivation strategy for efficient air-processed perovskite solar cells with excellent ambient stability. Solar Energy Materials and Solar Cells, 2021, 230, 111242.	6.2	23
62	Flower-like Ag coated with molecularly imprinted polymers as a surface-enhanced Raman scattering substrate for the sensitive and selective detection of glibenclamide. Analytical Methods, 2020, 12, 2858-2864.	2.7	22
63	Graphene oxide-based fluorescence molecularly imprinted composite for recognition and separation of 2,4,6-trichlorophenol. RSC Advances, 2015, 5, 2129-2136.	3.6	21
64	Preparation of anatase TiO2 microspheres with high exposure (001) facets as the light-scattering layer for improving performance of dye-sensitized solar cells. Journal of Alloys and Compounds, 2017, 694, 568-573.	5.5	21
65	Rapid and sensitive biomarker detection using molecular imprinting polymer hydrogel and surface-enhanced Raman scattering. Royal Society Open Science, 2018, 5, 171488.	2.4	21
66	2D/3D WO3/BiVO4 heterostructures for efficient photoelectrocatalytic water splitting. International Journal of Hydrogen Energy, 2021, 46, 27506-27515.	7.1	21
67	An isopropanol-assisted fabrication strategy of pinhole-free perovskite films in air for efficient and stable planar perovskite solar cells. Journal of Power Sources, 2017, 363, 317-326.	7.8	20
68	Au-Modulated Z-Scheme CuPc/BiVO ₄ Nanosheet Heterojunctions toward Efficient CO ₂ Conversion under Wide-Visible-Light Irradiation. ACS Sustainable Chemistry and Engineering, 2021, 9, 2400-2408.	6.7	20
69	Co-assembly of CdTe and Fe3O4 with molecularly imprinted polymer for recognition and separation of endocrine disrupting chemicals. Applied Surface Science, 2013, 284, 745-749.	6.1	19
70	Effect of calcination temperature on the microstructure of vanadium nitride/nitrogen-doped graphene nanocomposites as anode materials in electrochemical capacitors. Inorganic Chemistry Frontiers, 2019, 6, 164-171.	6.0	19
71	Green low-temperature-solution-processed in situ HI modified TiO2/SnO2 bilayer for efficient and stable planar perovskite solar cells build at ambient air conditions. Electrochimica Acta, 2019, 326, 134924.	5.2	19
72	Development of a model for predicting trihalomethanes propagation in water distribution systems. Chemosphere, 2006, 62, 1028-1032.	8.2	18

#	Article	IF	CITATIONS
73	In situ ligand-free growth of TiO2-escapsulated Au nanocomposites on photoanode for efficient dye sensitized solar cells. Chemical Engineering Journal, 2020, 396, 125302.	12.7	18
74	Photocatalytic Reduction of CO ₂ Using TiO ₂ -Graphene Nanocomposites. Journal of Nanomaterials, 2016, 2016, 1-5.	2.7	17
75	Tunable optoelectronic properties of D-A-Ï€-A type dyes by altering auxiliary acceptor position and atomic electronegativity. Journal of Molecular Liquids, 2019, 287, 110883.	4.9	17
76	Core–shell Ag-molecularly imprinted composite for SERS detection of carbendazim. International Journal of Environmental Analytical Chemistry, 2020, 100, 1245-1258.	3.3	17
77	A rational design of excellent light-absorbing dyes with different N-substituents at the phenothiazine for high efficiency solar cells. Spectrochimica Acta - Part A: Molecular and Biomolecular Spectroscopy, 2020, 234, 118241.	3.9	17
78	Graphene-modulated assembly of zinc phthalocyanine on BiVO ₄ nanosheets for efficient visible-light catalytic conversion of CO ₂ . Chemical Communications, 2020, 56, 4926-4929.	4.1	17
79	Ultrathin MnO2 nanosheets grown on hollow carbon spheres with enhanced capacitive performance. Physics Letters, Section A: General, Atomic and Solid State Physics, 2020, 384, 126539.	2.1	17
80	HI-assisted fabrication of Sn-doping TiO2 electron transfer layer for air-processed perovskite solar cells with high efficiency and stability. Solar Energy Materials and Solar Cells, 2020, 215, 110594.	6.2	17
81	Synthesis of multifunctional fluorescent magnetic graphene oxide hybrid materials. Journal of Colloid and Interface Science, 2012, 388, 9-14.	9.4	16
82	Self-assembled zeolitic imidazolate framework-8/Ag nanoparticles composite with well-controlled flower-like architectures for ultrasensitive surface-enhanced Raman scattering detection. Applied Surface Science, 2021, 537, 147853.	6.1	16
83	Gourmet powder functionalization of SnO2 for high-performance perovskite solar cells made in air. Electrochimica Acta, 2021, 371, 137812.	5.2	16
84	A theoretical study on the catalytic effect of nanoparticle confined in carbon nanotube. Chemical Physics Letters, 2011, 502, 96-100.	2.6	15
85	The preparation of hierarchical rutile TiO2 microspheres constructed with branched nanorods for efficient dye-sensitized solar cells. Journal of Alloys and Compounds, 2018, 747, 729-737.	5.5	14
86	Design and synthesis of a sandwiched silver microsphere/TiO2 nanoparticles/molecular imprinted polymers structure for suppressing background noise interference in high sensitivity surface-enhanced Raman scattering detection. Applied Surface Science, 2021, 544, 148879.	6.1	14
87	Sandwichâ€like Singledâ€Walled Titania Nanotube as a Novel Semiconductor Electrode for Quantum Dotâ€6ensitized Solar Cells. Advanced Energy Materials, 2012, 2, 639-644.	19.5	12
88	Metabolomics study on the cytotoxicity of graphene. RSC Advances, 2014, 4, 44712-44717.	3.6	12
89	Fabrication of nitrogen-rich three-dimensional porous carbon composites with nanosheets and hollow spheres for efficient supercapacitors. Inorganic Chemistry Frontiers, 2019, 6, 2082-2089.	6.0	12
90	Enhanced oxygen evolution performance by the partial phase transformation of cobalt/nickel carbonate hydroxide nanosheet arrays in an Fe-containing alkaline electrolyte. Inorganic Chemistry Frontiers, 0, , .	6.0	11

#	Article	IF	CITATIONS
91	Theoretical Analysis of Built-in Interfacial Electric Dipole Field in Dye-Sensitized Solar Cells. Journal of Physical Chemistry C, 2013, 117, 9092-9103.	3.1	10
92	Boosting the photoelectric conversion efficiency of DSSCs through graphene quantum dots: insights from theoretical study. Materials Chemistry Frontiers, 2021, 5, 5814-5825.	5.9	10
93	Aminoâ€Linked Conjugated Tetrazole Ring Passivation Strategy for Airâ€Processed Perovskite Cells with Predominant Stability and Efficiency. ChemSusChem, 2022, 15, .	6.8	10
94	Theoretical insights into the effect of pristine, doped and hole graphene on the overall performance of dye-sensitized solar cells. Inorganic Chemistry Frontiers, 2020, 7, 157-168.	6.0	9
95	Light harvesting enhancement by hierarchical Au/TiO2 microspheres consisted with nanorod units for dye sensitized solar cells. Solar Energy, 2020, 207, 592-598.	6.1	9
96	Core–shell Ag-dual template molecularly imprinted composite for detection of carbamate pesticide residues. Chemical Papers, 2021, 75, 3679-3693.	2.2	9
97	Degradation of Organic Pollutants in Water by Catalytic Ozonation. Chemical Research in Chinese Universities, 2007, 23, 273-275.	2.6	8
98	Mechanistic Understanding of Cetyltrimethylammonium Bromide-Assisted Durable CH ₃ NH ₃ Pbl ₃ Film for Stable ZnO-Based Perovskite Solar Cells. ACS Applied Energy Materials, 2020, 3, 9856-9865.	5.1	8
99	Construction and mechanistic understanding of high-performance all-air-processed perovskite solar cells <i>via</i> mixed-cation engineering. Materials Chemistry Frontiers, 2021, 5, 4244-4253.	5.9	7
100	Preparation of silver with an ultrathin molecular imprinted layer for detection of carbendazim by SERS. Chemical Papers, 2021, 75, 6477.	2.2	7
101	The sensing mechanism of pristine and transition metals doped Zn ₁₂ O ₁₂ , Sn ₁₂ O ₁₂ and Ni ₁₂ O ₁₂ nanocages towards NH ₃ and PH ₃ : a DFT study. Journal of Materials Chemistry C, 2021, 9, 17382-17391.	5.5	7
102	Elementary Photoelectronic Processes at a Porphyrin Dye/Singleâ€Walled TiO ₂ Nanotube Heteroâ€interface in Dye‧ensitized Solar Cells: A Firstâ€Principles Study. Chemistry - A European Journal, 2013, 19, 10046-10056.	3.3	6
103	Dummy molecular imprinted polymers coated with silver microspheres via surface enhanced Raman scattering for sensitive detection of benzimidazole. Spectrochimica Acta - Part A: Molecular and Biomolecular Spectroscopy, 2021, 249, 119321.	3.9	6
104	Modeling of residual chlorine in water distribution system. Journal of Environmental Sciences, 2003, 15, 136-44.	6.1	6
105	Active Functional Groups and Adjacent Dual-Interaction Strategies Enable Perovskite Solar Cells to Prosper: Including Unique Morphology and Enhanced Optoelectronic Performance. ACS Sustainable Chemistry and Engineering, 2022, 10, 9946-9955.	6.7	6
106	Coupled fluorescein isothiocyanate on graphene oxide. Materials Letters, 2011, 65, 751-753.	2.6	5
107	Hierarchical TiO ₂ microspheres composed with nanoparticle-decorated nanorods for the enhanced photovoltaic performance in dye-sensitized solar cells. RSC Advances, 2019, 9, 3056-3062.	3.6	5
108	Core-shell magnetic Ag-molecularly imprinted composite for surface enhanced Raman scattering detection of carbaryl. Journal of Environmental Science and Health - Part B Pesticides, Food Contaminants, and Agricultural Wastes, 2021, 56, 222-234.	1.5	5

#	Article	IF	CITATIONS
109	Specific iodide effect on surface-enhanced Raman scattering for ultra-sensitive detection of organic contaminants in water. Spectrochimica Acta - Part A: Molecular and Biomolecular Spectroscopy, 2022, 272, 120950.	3.9	5
110	Solvent-assisted preparation of low-temperature SnO ₂ electron transport layers for efficient and stable perovskite solar cells made in ambient conditions. New Journal of Chemistry, 2022, 46, 9841-9850.	2.8	5
111	Yb-doped SnO ₂ electron transfer layer assisting the fabrication of high-efficiency and stable perovskite solar cells in air. RSC Advances, 2022, 12, 14631-14638.	3.6	3
112	Grossly warped nanographene–phenothiazine nanocomposite as photoactive layer for solar cells: Insights from theoretical study. Chemical Physics Letters, 2021, 773, 138607.	2.6	1